Steady infiltration rate: Relation to antecedent soil moisture, soil permeability, and measurement method and period

Lucas Raimundo Rauber[(1)*] (ID), **Dalvan José Reinert**[(2)] (ID), **Paulo Ivonir Gubiani**[(2)] (ID) **and Suelen Matiasso Fachi**[(1)] (ID)

[(1)] Universidade Federal de Santa Maria, Programa de Pós-Graduação em Ciência do Solo, Santa Maria, Rio Grande do Sul, Brasil.
[(2)] Universidade Federal de Santa Maria, Departamento de Solos, Santa Maria, Rio Grande do Sul, Brasil.

* Corresponding author:
E-mail: lucas.rauber@ufsc.br

ABSTRACT: Soil steady water infiltration rate (SIR) is a key variable in hydrological modeling, but its relationship to antecedent soil moisture is not yet well understood. We tested the hypothesis that the SIR decreases with the increase in antecedent moisture, and that this relationship depends on permeability to water on the soil surface, the measurement method, and the measurement period. We conducted an experiment in an *Argissolo Vermelho-Amarelo Distrófico abrúptico* (Psammentic Paleudult – Soil Taxonomy), measuring infiltration in up to 14 antecedent moisture conditions under two soil structural conditions (no-till and no-till with subsoiling), with two measurement methods (double ring and Cornell infiltrometers), and for up to 48 h, with ten replications. In addition, vertical effective hydraulic conductivity of the saturated profile (Kef) was determined with Darcy's equation for N layers. Crop succession used in the area was black oats and ryegrass in the winter and soybean in the summer. The SIR decreased to as little as 7.7 % of its original value with the increase in antecedent moisture; it was ~200 % greater in the treatment with subsoiling compared to no-till alone, and ~80 % greater when measured with the Cornell infiltrometer than with the double ring infiltrometer. Nevertheless, the effects of the method and the soil structural condition declined with the increase in antecedent moisture, confirming our hypothesis. In soil initially nearly saturated (degree of saturation ~90 %), the SIR drew near Kef (12.7 mm h^{-1}) under the two soil structural conditions, especially when measured with the double ring infiltrometer. In contrast, increasing the time for measuring infiltration (>2 h) did not generate a new lower SIR level. The SIR decreases with the increase in antecedent soil moisture, and this relationship depends on the permeability to water of the surface layers and the measurement method. The SIR determined with infiltrometers better corresponds to vertical infiltration the nearer the soil is to saturation before beginning measurement.

Keywords: surface runoff, double ring infiltrometer, Cornell infiltrometer, terraces, lateral flow.

INTRODUCTION

Steady infiltration rate (SIR) of water into the soil is defined as the final value of the infiltration curve that occurs in a vertical and homogeneous column, and that numerically draws near the hydraulic conductivity of the saturated soil (Hillel, 2003). It is a key hydrological value, and it must be appropriately characterized to design soil and water conservation projects (e.g., terraces) (Pruski et al., 1997), irrigation projects (Assouline, 2013), and civil engineering works (e.g., septic tanks for wastewater) (Fepam, 2019). However, in spite of the hydrological importance of water infiltration into the soil, it is not sufficiently clear whether antecedent moisture in the soil affects the SIR.

According to the boundary conditions and assumptions used to define the SIR (e.g., vertical and homogeneous column, a sufficient time for the flux density to reach the hydraulic conductivity of the saturated soil), it would not be affected by the antecedent soil moisture (Philip, 1957, 1969; Hillel, 2003). However, experimentally, Císlerová et al. (1988) found an inverse relationship between the SIR and antecedent moisture. In another study, Liu et al. (2019) found that although antecedent moisture predominantly affects the initial rates of the infiltration curve, the effect is also propagated in the SIR. Furthermore, other authors (Boeno et al., 2021; Rauber et al., 2021; Wei et al., 2022) have suggested more detailed investigation of the relationship between the SIR and antecedent soil moisture.

A relationship between antecedent moisture and the SIR seems to be more evident in point infiltration measurements with infiltrometers (Rauber et al., 2021) than in plot-scale measurements (Bertol et al., 2015). Furthermore, this relationship may depend on the soil surface water permeability, the method used, and the measurement period. Although the infiltration rate measured in the field with infiltrometers tends to exhibit a stable infiltration rate, the tests may not ensure the boundary conditions used in the conceptual definition of the SIR, such as the homogeneous structure of the porous medium in space and time and, above all, a solely vertical flow (Hillel, 2003).

In a stratified soil profile with respect to water permeability, the lateral flow in infiltration measured with infiltrometers (Boeno et al., 2021) may be strengthened when the wetting front reaches more restrictive subsurface layers, especially if the single-ring measurement method is used (e.g., Cornell infiltrometer). In double ring infiltrometers, the outer ring is used to attenuate the lateral flow coming from the inner ring (in which measurements are taken) (Bouwer, 1986). The capacity of the outer ring to attenuate the flow coming from the inner ring, however, may depend on the antecedent soil moisture. Another problem is that the measurement time with infiltrometers (2 to 3 h) may be insufficient to saturate the soil profile and incorporate the hydraulic resistance of deep soil layers less permeable to water in the SIR. For example, even if the SIR has stabilized within an initial measurement interval (e.g., in the last 20 min of a 2-h test), increasing the measurement time may generate a new lower level of the SIR if the wetting front reaches more restrictive deep layers (Boeno et al., 2021). However, experimentation is necessary to study how antecedent moisture, the permeability to water of the soil surface, the type of infiltrometer, and measurement time may affect lateral infiltration and, consequently, the SIR.

Studying the relationship between antecedent moisture and infiltration is experimentally challenging. In addition to the effect of antecedent moisture on infiltration variables, there is the space-time effect of dynamic factors such as the number and type of roots (Bodner et al., 2008; Cui et al., 2019; Liu et al., 2019) and change in the intensity and seasonal frequency of wetting and drying cycles, factors that affect the macroporosity and water flow in the soil (Bodner et al., 2013; Castiglioni et al., 2018). These factors can make the relationship between antecedent moisture and the SIR confusing (Rauber et al., 2021).

To better investigate the relationship between antecedent moisture and the SIR, measuring infiltration at various times of the year with contrasting antecedent moisture conditions is important, which would allow the determination of the contribution of antecedent moisture to temporal variability of the SIR. In addition, establishing expressive variation in antecedent moisture over a short period (e.g., with irrigation) would make it possible to minimize seasonal effects on the relationship between antecedent moisture and the SIR.

Due to their practicality and low cost, infiltrometers are the methods generally used to characterize infiltration variables (Lili et al., 2008; Rahmati et al., 2018). Therefore, understanding how the SIR measured by these devices is affected by antecedent moisture may have relevant implications, such as delimitation of the most suitable antecedent moisture conditions for minimizing lateral infiltration. For example, measuring the SIR under low antecedent moisture may lead to overestimation of vertical infiltration and to undersizing works to contain water surface runoff, such as terraces.

We hypothesized that the SIR measured with infiltrometers decreases with an increase in antecedent soil moisture, and that this relationship depends on the permeability to water of the soil surface, on the measurement method, and on the measurement period. This study aimed to test whether the SIR measured with infiltrometers decreases with an increase in antecedent soil moisture, and whether this relationship depends on the permeability to water of the soil surface and on the measurement method and measurement time.

MATERIALS AND METHODS

Study location and experimental design

The experiment was conducted in the area of the Soil Department of the Universidade Federal de Santa Maria, Rio Grande do Sul State, Brazil (29° 43' 11'' S, 53° 42' 12'' W, altitude of 86 m), in a soil classified as *Argissolo Vermelho-Amarelo Distrófico abrúptico,* according to the Brazilian classification system (Santos et al., 2018), and as a Psammentic Paleudult, according to the North American classification system (Soil Survey Staff, 2022). Surrounding topography is slightly rolling. Slope at the experiment site is 6 % (± 0.70 %). Soil source material at the site is sedimentary (clayey siltstone). Main minerals are kaolinite (predominant), vermiculite, goethite, and hematite (Pedron et al., 2018). Historical mean annual rainfall is 1,700 mm (information obtained from the database of the INMET meteorological station at a distance of ~1,600 m from the experiment in this study). The local climate is Cfa according to the Köppen classification system.

The experiment was set up in 2021 in a representative long-term no-till area (~20 years) with intercropping of oats (*Avena sativa*), ryegrass (*Lolium multiflorum*), and radish (*Raphanus sativum*) in the winter, and soybean (*Glycine max*) or corn (*Zea mays*) in the summer. The study factors evaluated were (i) moisture conditions prior to measurement of infiltration (13 for the Cornell infiltrometer and 14 for the double ring infiltrometer), (ii) two soil structural conditions (no-till – NT, and no-till with subsoiling – Sub), (iii) two methods of measuring infiltration (Cornell infiltrometer and the double concentric ring infiltrometer), and (iv) duration of the infiltration tests (1 h for the Cornell infiltrometer and from 2-48 h for the double ring infiltrometer). The experiment was organized in split plots.

The experimental area, 30 × 20 m (600 m²), was initially divided into two to delimit the two soil structural conditions. After that, one of the two parts was subsoiled on April 30, 2021, when the soil had a friable consistency, with moisture of 0.09 g g^{-1} in the 0.00-0.10 and 0.10-0.20 m layers and of 0.10 g g^{-1} in the 0.20-0.30 m layer. To obtain intense soil mobilization and promote a considerable increase in the permeability to water in the subsoiled layer, subsoiling was performed in one direction and then in a direction

perpendicular to the first, using a 5-shank subsoiler operating to a depth of ~0.40 m. Infiltration was evaluated from 3.2 to 20.5 months after subsoiling.

Soil moisture monitoring

In both soil structural conditions, soil moisture was continuously monitored with FDR (Frequency Domain Reflectometer) sensors, model CS616, with 30-cm probe rod length. Calibration equations of the probes (relationship between period recorded by the probe and corresponding volumetric moisture) for the soil layers of 0.00-0.10 m (Equation 1), 0.10-0.30 m (Equation 2), and 0.30-0.60 m (Equation 3), and the E horizon (Equation 4) and Bt horizon (Equation 5) are shown below. These equations were calibrated and validated for the same soil and experimental area of this study (Rauber, 2023).

$$\theta = 9.946 - 1.946T + 0.1396T^2 - 0.004356T^3 + 0.0000506T^4 \tag{Eq. 1}$$

$$\theta = 14.87 - 2.872T + 0.2048T^2 - 0.006399T^3 + 0.00007461T^4 \tag{Eq. 2}$$

$$\theta = 9.865 - 1.971T + 0.1445T^2 - 0.004624T^3 + 0.00005517T^4 \tag{Eq. 3}$$

$$\theta = 18.94 - 3.598T + 0.2538T^2 - 0.007892T^3 + 0.00009194T^4 \tag{Eq. 4}$$

$$\theta = -4.114 + 0.5221T - 0.02197T^2 + 0.0003227T^3 \tag{Eq. 5}$$

in which: θ is the volumetric soil moisture (m³ m⁻³) and T is the period recorded by the FDR probe (µSec). All the coefficients of the equations were significant ($p < 0.01$).

To set up the probes in the soil profile, pits were opened, and in three locations of each one of the two soil structural conditions, the CS616 probes were horizontally inserted at the depths of 0.025, 0.075, 0.15, 0.30, and 0.50 m, which represent the center of the soil layers of 0.00-0.05, 0.05-0.10, 0.10-0.20, 0.20-0.40, and 0.40-0.60 m, respectively. These layers were considered morphologically different from each other based on the structural characteristics (aggregate form and resistance to knife insertion into the profile). Soil water storage (SWS) in each layer was obtained by the product between volumetric moisture and the thickness of the layer. Water storage in the vertical section of the profile with two or more layers was determined by equation 6:

$$SWS = (\theta i_1 * dz_1) + (\theta i_2 * dz_2) + \cdots (\theta i_n * dz_n) \tag{Eq. 6}$$

in which: θi represents the soil moisture in the center of the layer (L³ L⁻³) and dz is the thickness of each soil layer (L). The indices 1, 2, ..., n represent the soil layers from the top to the bottom of the soil layer.

In addition, at a fourth point in each soil structural condition, 18 probes were set up at the depths of 0.00625, 0.025, 0.05, 0.075, 0.10, 0.125, 0.15, 0.175, 0.21, 0.25, 0.30, 0.35, 0.40, 0.45, 0.50, 0.56, and 0.68 (E horizon), and 0.85 m (Bt horizon). The greater discretization of the soil profile at this point served to monitor the advance of the wetting front in greater detail in the infiltration tests performed over the probes (discussed below).

Each layer and horizon taken from the soil during the opening of the pits was placed separately to the side of each profile. After setting up the probes, the soil taken from opening the pit was returned to it, maintaining the same initial arrangement of the layers and horizons. In addition, each layer was carefully compacted (by trampling) to approximately reestablish the initial degree of soil compaction. The probes were connected to a CR1000 datalogger and to an AM16/32 multiplexer. The programming was set to record and store data every hour. The systems were reprogrammed for continuous recording of

moisture every minute to monitor moisture during the infiltration tests performed over the probes (discussed below).

Determination of infiltration

Under different antecedent moisture conditions, soil water infiltration was determined with a Cornell infiltrometer (hereafter "Cornell") and a double concentric ring infiltrometer (hereafter "double ring") under both soil structural conditions. Ten infiltration determinations were made for each combination of soil structural condition, antecedent moisture, and measurement method. The measurement locations were demarcated to be equidistant (3 m), and the successive measurements at each point with different antecedent moisture conditions were always made at the same demarcated locations. There was no machine traffic over the area throughout the period of the study (04/2021 to 02/2023). Winter crop (oats + ryegrass) was broadcast sown, and the summer crop (soybean) was sown in rows (0.45 m spacing), both sown manually.

Infiltration tests with the double ring (Bouwer, 1986) lasted two hours and were carried out with a constant hydraulic pressure head of 0.03 m. The outer rings (0.40 m diameter and 0.10 m height) and inner rings (0.20 m diameter and 0.15 m height) were inserted into the soil to a depth of 0.05 and 0.075 m, respectively. The infiltration measurements were made at 2 to 3-minute intervals at the beginning (0-10 min) and 10-min intervals for the remainder of the test. The SIR was considered the mean of the last two to three stable values of the infiltration rate.

Infiltration tests with the Cornell (Ogden et al., 1997; van Es and Schindelbeck, 2003; Seratto et al., 2019) lasted approximately one hour, which corresponded to the time for the depletion of the water from the infiltrometer under the application rate of ~300 mm h^{-1}; the infiltrometers were previously adjusted for this precipitation rate. Rings of 0.25 m diameter and 0.15 m height were inserted into the soil to a depth of 0.075 m. Readings of the water application rate and surface runoff rate were taken every 3 min. Infiltration rate was calculated by the difference between the water addition rate and the surface runoff rate. The SIR was considered the mean of the last two to three stable values of the infiltration rate.

In both soil structural conditions, the infiltration tests were carried out in 13 (Cornell) and 14 (double ring) antecedent moisture conditions in the period from 08/2021 to 01/2023 (Figure 1). A wide range of antecedent moisture conditions before the soil natural wetting and drying cycles was analyzed. For example, the degree of saturation of the 0.00-0.40 m layer before the infiltration tests ranged from approximately 40 to 90 %, which represents a wide variation of moisture around field capacity, whose corresponding degree of saturation is ~63 %. The mean time between the measurements under different moisture conditions was 38 days (±11 days) for the double ring and 40 days (±7 days) for the Cornell (Figure 1). In spite of the nearly regular frequency of measurement, the dates were defined to have antecedent soil moisture different from the previous date. Air temperature and rainfall during the experimental period are shown in figure 1. Natural annual rainfall was 1,420 mm in 2021 and 1,536 mm in 2022 (annual accumulation below the historic mean of 1,700 mm). In addition, the irregularity in the rainfall distribution throughout the period (for example, greater water scarcity from 10/2021 to 03/2022 – Figure 1) contributed to obtain infiltration variables over a wide range of antecedent moisture conditions.

Due to the low frequency of rainfall events able to saturate or nearly saturate the soil, irrigation was used on one of the evaluation dates (September 21, 2022) so that infiltration could be measured under nearly saturated soil conditions. The total area of each soil structural condition was initially irrigated (until the moisture in the profile reached maximum values), and the infiltration tests were immediately carried out.
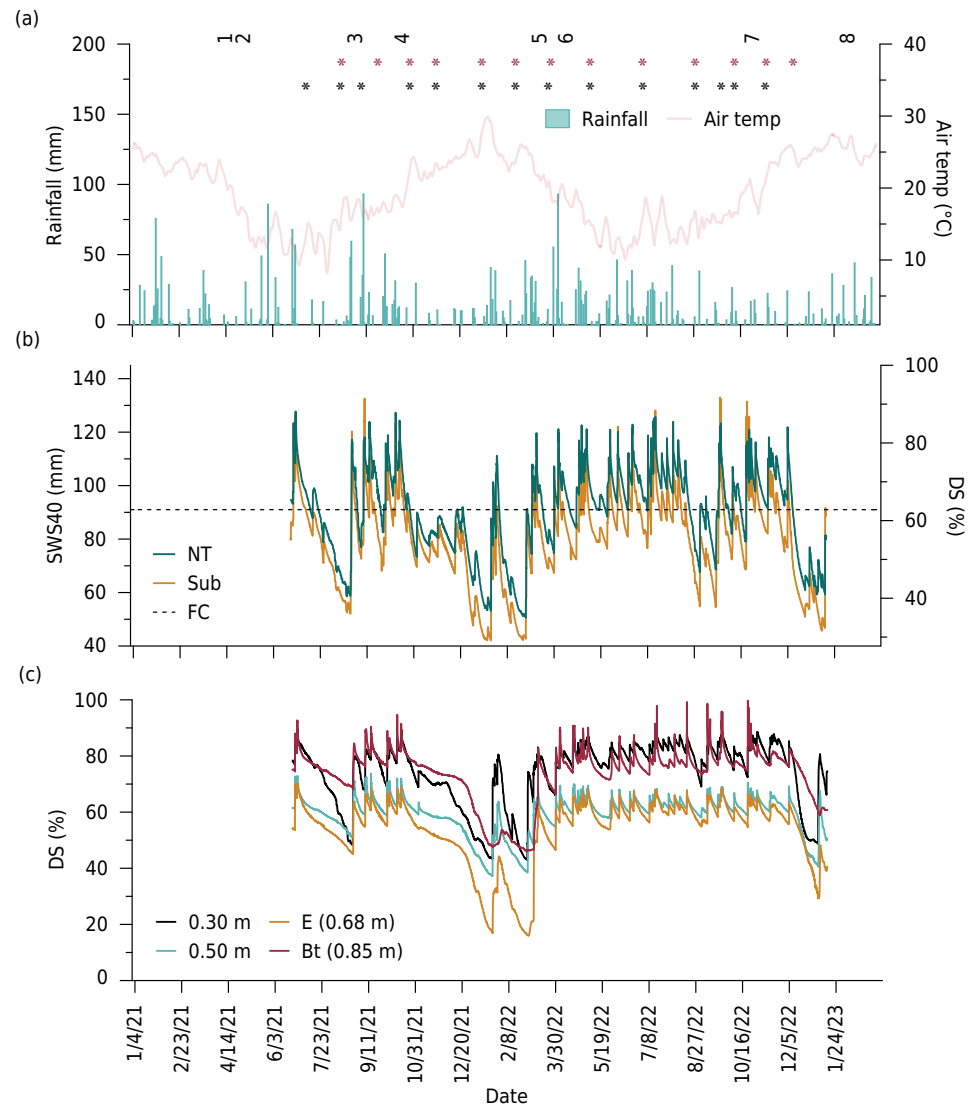
Figure 1. Mean daily air temperature (Air temp) (10-day moving mean) and cumulative rainfall of each natural rainfall event throughout the experimental period (a); water storage in the 0.00-0.40 m layer (SWS40) and corresponding degree of saturation (DS) in no-till (NT) and no-till with subsoiling (Sub) areas (b); DS at different depths of the soil profile in a no-till area (c). In figure "a", asterisks in red and in black refer to the dates of infiltration assessment using the Cornell infiltrometer and the double ring infiltrometer, respectively. The numbers (1 to 8) in figure "a" indicate the position (date) of different management operations carried out in the area: 1 – subsoiling, 2 – sowing of oats + ryegrass, 3 – first soil collection, 4 – soybean sowing, 5 – second soil collection, 6 – sowing of oats + ryegrass, 7 – soybean sowing, 8 – third soil collection. Rainfall and temperature data were obtained from an INMET meteorological station at a distance of ~1,600 m from the experiment. FC: field capacity (10 kPa) (mean value).

Infiltration rate after extending the measurement time

To analyze the response of the infiltration rate upon extending the measurement time beyond 2 h (the maximum time of the measurements described above), infiltration tests over a 48-h period were carried out with the double ring under each soil structural condition (setting up the rings and hydraulic pressure head described above). These tests were carried out on October 01, 2021 and April 19, 2022, with three to five replications. On the first and second assessment dates, the antecedent soil moisture expressed by storage in the 0.00-0.40 m layer was above (12 %) and below (13 %) field capacity, respectively. The infiltration rate was measured manually at approximately 2-min intervals at the beginning of the test (0-10 min), every 10 min up to the 2-h duration, and every 10 min from 23-24 h and from 47-48 h. The effect of extending the measurement time

was analyzed, comparing the mean infiltration rate obtained in each time interval. To maintain the hydraulic pressure head in the infiltration rings in the time intervals in which infiltration was not being monitored (i.e., from 2-23 h and from 24-47 h), floats to regulate the level were used in the outer ring, connected by a hose to a water reservoir of approximately 10,000 liters at the highest level of the area. A siphon was used to transfer water from the outer ring to the inner ring, thus maintaining the same water level in both.

On each assessment date and under each soil structural condition, one of the replications was placed where the FDR moisture monitoring sensors with high-profile discretization (18 probes) had been placed. Time intervals for reading infiltration after two hours were shorter at these points than at the other points. Readings were more discretized to better detect the relationship between the infiltration rate and the advance of the wetting front monitored with the FDR sensors that were installed below the projection of the rings and that monitored soil moisture every minute.

Changes in point infiltration resulting from additional soil moistening through irrigation

To try to isolate the effect of antecedent moisture on the SIR in the face of possible autocorrelated seasonal effects (e.g., changes in soil structure, pore obstruction by roots), the total area of the soil was wetted with an irrigation system (at intervals of up to two days) with concomitant assessment of the SIR. For example, the aim was to analyze whether expressive changes in antecedent moisture in a short period of time would change the SIR, or if successive soil-wetting cycles would be necessary to significantly decrease the SIR.

Initial infiltration tests at five points under each soil structural condition were carried out, of 2-h duration, on October 21, 2022. The initial degree of soil saturation in the 0.00-0.40 m layer was 51 % (mean between the soil structural conditions). One point in each soil structural condition was placed over the high discretization moisture monitoring profile (18 probes). After the end of the tests, the total area of the experiment was immediately irrigated for 3.3 h, for cumulative precipitation of ~155 mm. The constant intensity of the precipitation (47 mm h^{-1}) corresponded to the maximum intensity obtained from the irrigation system, and it was enough to nearly saturate the soil. Infiltration was once more evaluated immediately after irrigation, at the same points, for approximately 1 h. On 22 and 24 Oct. 2022, infiltration was once more evaluated, also under previous moistening of the total area of soil with the irrigation system for 1 h. On October 26, 2022, infiltration was also evaluated, but with moistening of the soil in the total area after finishing the tests. Finally, on October 28, 2022, infiltration was evaluated once more, but without prior or subsequent irrigation of the area. Soil moisture below (high discretization profiles) and beside (other moisture profiles) the infiltration rings was monitored every 1 min over the period. The irrigation system consisted of 180° SempreVerde/Fabrimar sprinklers well distributed across the area. Collection cups were distributed in the area to measure the irrigation depth and the precipitation rate. The water drops fell from a height of ~2.5 m.

Determination of soil physical properties

Hydraulic conductivity of the saturated soil and soil bulk density and pore distribution were determined according to the methodology described in Teixeira et al. (2017) on September 16, 2021, April 01, 2022, and February 24, 2023, which corresponded to 4.6, 11.2, and 22.2 months since subsoiling, respectively. Stainless steel rings with diameter of 6 cm and height of 4 cm were used to collect undisturbed samples in the 0.00-0.05, 0.05-0.20, 0.20-0.40, and 0.40-0.60 m layers using ten replications distributed in two soil profiles opened in each soil structural condition. The rings were inserted vertically into each soil layer. Furthermore, on September 16, 2021, 20 samples per horizon

(E, Bt1, and Bt2) were collected in a soil profile representative of the area, disregarding the effect of the soil structural condition. The purpose of this was to determine some physical hydric characteristics of the subsurface pedogenetic horizons.

In the laboratory, all the samples were saturated by capillarity and evaluated for hydraulic conductivity of the saturated soil under a constant hydraulic pressure head of 0.02 m. Subsequently, the samples were placed under tensions of 1, 6, and 10 kPa on a sand tension table (Reinert and Reichert, 2006) and 100 kPa in a Richards pressure chamber to determine pore distribution (Teixeira et al., 2017). Finally, the samples were dried in a laboratory oven for 48 h to determine soil bulk density. Total porosity was determined by the relationship between soil bulk density and particle density (2.61 Mg m^{-3}). Field capacity was attributed to moisture corresponding to the tension of 10 kPa (Teixeira et al., 2017). With the mean hydraulic conductivity of the saturated soil of each layer, time period, and soil structural condition, the effective vertical hydraulic conductivity of the saturated profile (Kef) was determined according to Darcy's equation for N layers (Equation 7):

$$Kef = \frac{Z}{\left[\frac{dz1}{K1} + \frac{dz2}{K2} + \frac{dz3}{K3} + \cdots \frac{dzn}{Kn}\right]}$$

Eq. 7

in which: Z is the depth of the profile (L), dz is the thickness (L), and K (L T^{-1}) is the hydraulic conductivity of the saturated soil of each layer, represented by the indices 1, 2, ..., n. The thicknesses of the soil layers and horizons are shown in table 1. The Kef estimate was made considering an effective soil profile depth of 1.4 m.

Hydrological characteristics of the soil

The mean Kef between the two soil structural conditions and the three evaluation times was 12.7 mm h^{-1} (± 4.7 mm h^{-1}), which is relatively low (Table 1). For example, considering the four soil hydrological groups (scale from A to D) used to estimate excess rain by the curve number method adapted to Brazil (Sartori et al., 2005a,b), the soil of this study fits in Group C. Group A represents soils with low surface runoff potential, whereas Group D represents soils with high surface runoff potential. The main characteristic that determines the relatively high risk of surface runoff in this soil is the low permeability to water of the 0.20-0.40 m layer and of the Bt horizon (Table 1). In addition, these layers remain with a relatively high degree of water saturation compared to the other layers throughout most of the year (Figure 1c), which generates a low hydraulic gradient for water infiltration into the soil.

Table 1. Physical hydric characteristics of the studied soil (Argissolo Vermelho-Amarelo Distrófico abrúptico)

Hz	Layer	Total sand	Corse sand	Fine sand	Silt	Clay	Ksat[1]	
							NT	Sub
	m			g kg^{-1}			mm h^{-1}	
Ap	0.00-0.05	648	239	409	262	90	134	218
A1	0.05-0.20	624	230	394	268	108	21	191
	0.20-0.40						4	11
A2	0.40-0.60	586	176	410	293	121	29	19
E	0.60-0.80	604	164	440	341	55	35[2]	
Bt1	0.80-0.90	525	144	381	347	128	8[2]	
Bt2[3]	0.90+	417	128	289	290	293	15[2]	

Hz: horizon; Ksat: hydraulic conductivity of the saturated soil (mean of the three collection dates); [1] NT – no till; Sub – no till with subsoiling; [2] Mean values in each horizon; [3] Thickness of at least 0.50 m.

Statistical analysis

The Pearson Correlation between the infiltration and antecedent moisture variables was initially carried out to detect which variable representing soil moisture prior to the infiltration tests would be better correlated with the SIR. Results indicated better correlation between the SIR and water storage of the 0.00-0.40 m layer (SWS40). Subsequently, linear regression analysis SIR = f (SWS40) was carried out for each soil structural condition and infiltration measurement method. The effect of extending the measurement time (2, 24, and 48 h) in the SIR measured with the double ring was analyzed with analysis of variance (ANOVA), followed by comparison of means by Tukey's test (p<0.05) for each date and soil structural condition. ANOVA, followed by comparison of means by Tukey's test (p<0.05), was carried out for each soil structural condition to analyze the effect of the SIR evaluation period, concomitant with additional moistening of the soil through irrigation. Furthermore, the effect of soil moisture variables at different infiltration stages (mean infiltration rate in the periods of 0-10, 10-30, 30-60, 60-90, and 90-120 min) and in cumulative infiltration was analyzed through ANOVA, followed by linear regression. The effect of the soil structural condition and of the measuring period on bulk density, pore size distribution, and hydraulic conductivity of the saturated soil was analyzed through ANOVA, followed by multiple comparison of means by Tukey's test (p<0.05). The assumptions of the analyses of variances were appropriately checked and met. All the statistical procedures were carried out in the R environment (R Development Core Team, 2022).

RESULTS

Significant linear association between the SIR and SWS40 was found, in which the angular regression coefficient was dependent on the soil surface permeability to water and on the measurement method (Figure 2). The SIR was ~200 % greater in the treatment with subsoiling compared to no-till, and ~80 % greater when determined with the Cornell compared to the double ring (Figure 2). However, the effect of surface permeability and of the measurement method on the SIR decreased with an increase in SWS40. With antecedent moisture near saturation (degree of saturation of ~90 %), and especially in the evaluations with the double concentric ring, the SIR in the two soil structural conditions tended to exhibit minimum values, near the Kef (12.7 mm h^{-1}) (Figure 2). In contrast, for the same antecedent moisture (above or below field capacity), extending the test from 2 to 24 h and 48 h did not create a new lower level of the SIR and nearness to Kef (Figure 3), although it was enough for the vertical infiltration flow to reach subsurface layers of difficult permeable, such as the 0.20-0.40 m layer and the Bt horizon (Figure 4).

DISCUSSION

The results of this study confirmed the hypothesis that the SIR decreases with an increase in antecedent moisture and that this relationship depends on the permeability to water of the soil surface and on the measurement method. However, the hypothesis that there would be an effect from the extension of the measurement time on the SIR (e.g., a new lower SIR level) was rejected. The results also suggest that measuring infiltration with infiltrometers does not ensure the boundary conditions used to define the SIR (e.g., homogeneous structure and solely vertical flow), and they suggest that antecedent moisture is a key variable that must be characterized to complement measurement of the SIR with infiltrometers.

The effect of antecedent moisture on the SIR in this study (Figure 2) was greater than that found experimentally by other authors. For example, Cui et al. (2019) found that for a silty soil in China, the SIR was more greatly affected by the weight of fine roots than by the antecedent soil moisture. To determine infiltration, the authors used a method of constant water supply on the soil, which consists of measuring infiltration according

to the advance of the wetted area, assisted by a digital camera. The SIR was obtained at 75 min of testing. A study conducted in a *Cambissolo Húmico* in a natural highland pasture area in the south of Brazil found correlation of only -0.39 between gravimetric antecedent moisture (0.00-0.20 m layer) and the SIR measured with a double ring (Rauber et al., 2021). The demarcation of fixed points to assess infiltration in this study may have made it possible to isolate the effect of antecedent moisture on the SIR better than the other reported studies did. The coefficients of determination (0.52 to 0.74) of the relationship between antecedent moisture and the SIR in this study (Figure 2) show that for the same method and soil structural condition, antecedent soil moisture explains most of the temporal variability of the SIR.

The increase in the initial infiltration rate and in the cumulative infiltration as a result of reduction in antecedent moisture is in accordance with the increase in the initial hydraulic gradient and in the degree of opening of the macropores (Cui et al., 2019; Liu et al., 2019; Yang et al., 2020; Wei et al., 2022). This is corroborated by the higher angular coefficient (in modulus) of the antecedent moisture with the initial infiltration rates than with the SIR. However, the significant effect of antecedent moisture on the SIR is noteworthy (Figure 2). For example, for the double ring method and the subsoiled area, the SIR obtained for the lowest antecedent moisture (degree of saturation of ~40 %) was ~13 times greater than the SIR obtained under soil that was initially nearly saturated (Figure 2). For the same soil and experimental area as this study, Boeno et al. (2021) estimated that 90 % of the SIR obtained with the double ring (no-till area; antecedent soil moisture around field capacity) came from the lateral component of infiltration. However, that study did not measure the effect of antecedent moisture on the magnitude of lateral flow. This study shows displacement across the entire length of the infiltration curve obtained experimentally with infiltrometers as the antecedent moisture changes. For example, higher antecedent moisture decreased the infiltration rate of all the stages of the infiltration curve.
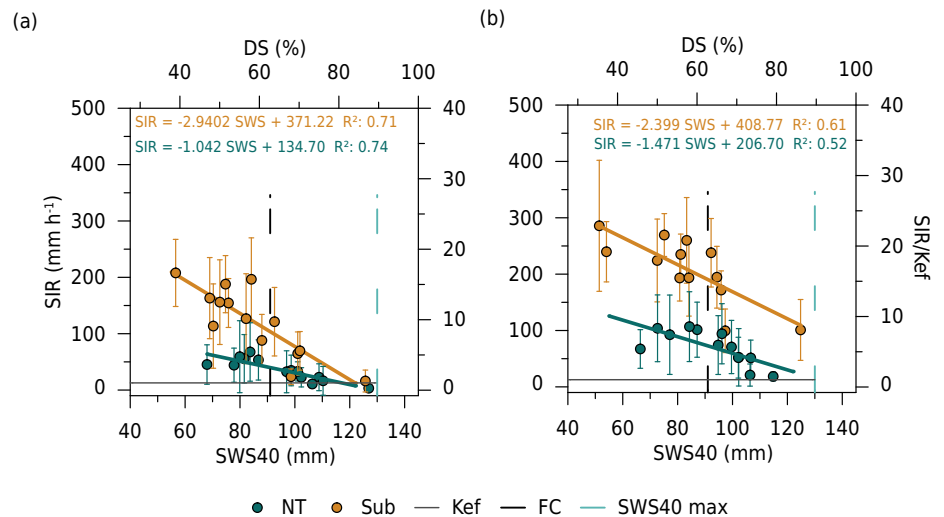

Figure 2. Relationship between antecedent soil moisture and the steady infiltration rate (SIR) measured with the double ring infiltrometer (a) and the Cornell infiltrometer (b) in a no-till (NT) area and in a no-till with subsoiling (Sub) area. Each point on the graphs represents the mean of ten replications. Error bar represents the standard deviation (spatial variability of infiltration). SWS40: water storage in the 0.00-0.40 m soil layer prior to the infiltration tests. Kef: effective vertical hydraulic conductivity of the saturated profile determined using equation 7 (mean value). SIR/Kef: relationship between the SIR and Kef. FC: field capacity (-10 kPa) (mean value). SWS40 max: maximum water storage observed in the 0.00-0.40 m layer throughout the experimental period (mean value between the soil structural conditions). DS: degree of saturation by water corresponding to water storage in the 0.00-0.40 m soil layer.
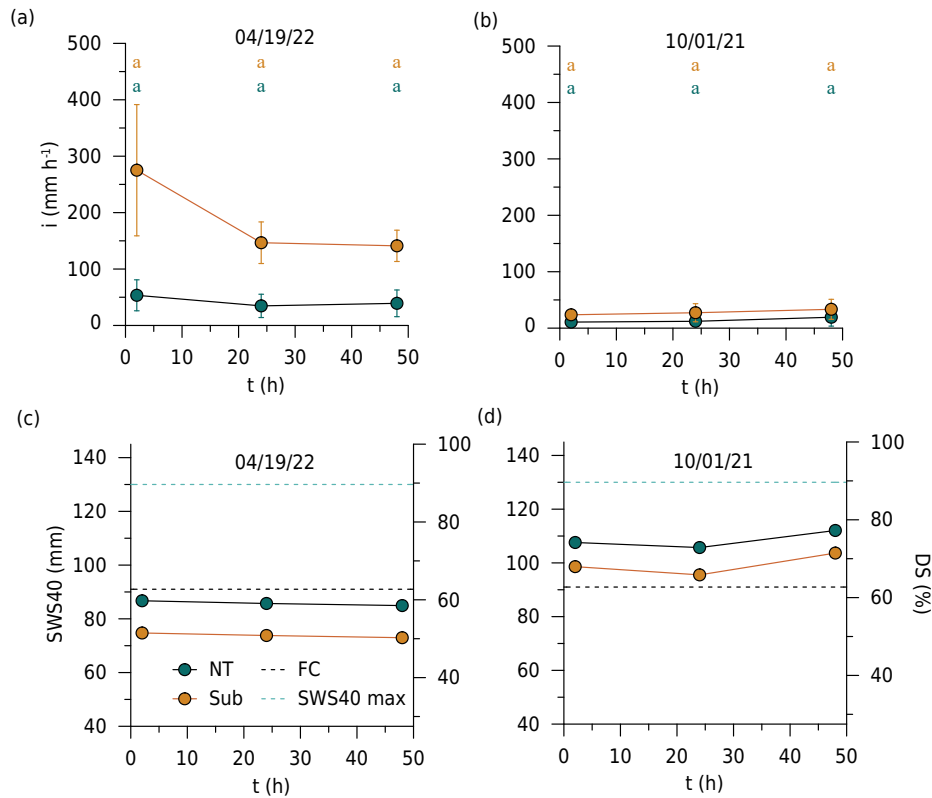
Figure 3. Water infiltration rate into the soil (i) determined with the double concentric ring infiltrometer at 2, 24, and 48 h after the beginning of the infiltration test under different soil structural conditions and assessment dates (a, b), and the respective antecedent soil moisture (c, d). NT: no-till. Sub: no-till with subsoiling. SWS40: water storage in the 0.00-0.40 m soil layer lateral to the infiltration points (outside of the projected flow area below the projection of the rings). FC: field capacity (-10 kPa) (mean value); SWS40 max: maximum water storage observed in the 0.00-0.40 m layer throughout the experimental period (mean value between the soil structural conditions); DS: degree of saturation by water corresponding to water storage in the 0.00-0.40 m soil layer. For each soil structural condition and date, mean values with different letters (green for NT and orange for Sub) statistically differentiate the assessment periods by Tukey's test (p<0.05). Error bar in the infiltration graphs (a, b) represents the standard deviation.
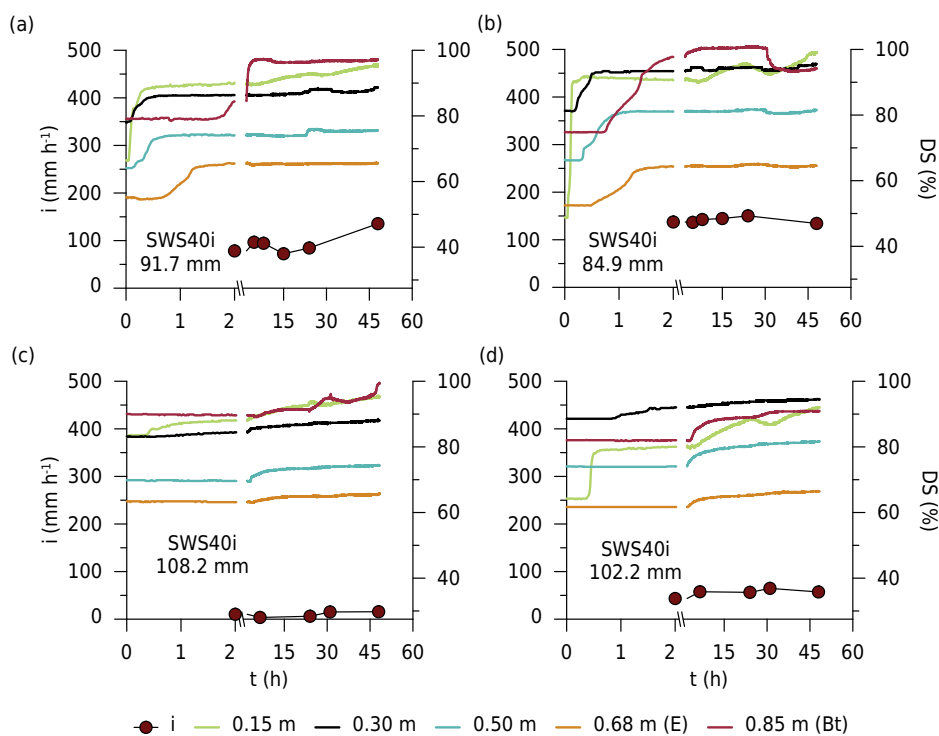
Figure 4. Water infiltration rate (i) determined with the double concentric ring infiltrometer and degree of saturation (DS) at different soil layers below the projection of the rings during the long-term infiltration tests (up to 48 h) in soil under no-till (a, c) and no-till with subsoiling (b, d). SWS40i: Initial water storage in the 0.00-0.40 m layer.

Soil pore distribution was not clearly affected by the evaluation time. The effects of subsoiling on soil structure, which are generally temporary (Drescher et al., 2016), were maintained for at least 22 months in this study. Seasonal changes in soil structure that could obscure the relationship of antecedent moisture with the SIR (Rauber et al., 2021) were, therefore, not observed in this study. Nevertheless, changes in the level of pore obstruction by roots may have occurred between the time periods. In any case, the SIR decreased significantly due to the quite sudden increase in soil moisture below and beside the projection of the infiltration rings through additional wetting of the soil with irrigation. That reinforces a direct and important effect of antecedent moisture on the SIR. For example, during the short time interval in which these tests with additional wetting of the soil were carried out (i.e., interval of up to 5 h between the beginning of irrigation and subsequent evaluation of the SIR), there was probably no change in soil structure and/or in the level of pore obstruction by roots. The results also suggest there is no need for several successive soil moistening cycles to significantly decrease the SIR.

The reduction in antecedent soil moisture increased the amplitude of the difference in the SIR between the soil structural conditions (Figure 2). That shows infiltration becomes more dependent on the permeability to water of the surface layers as the antecedent moisture decreases. Subsoiling, for example, led to a ~9-fold increase in hydraulic conductivity of the saturated soil in the 0.05-0.20 m layer (Table 1), which may have increased lateral infiltration, although we did not directly measure whether the horizontal hydraulic conductivity is similar to the vertical hydraulic conductivity (degree of anisotropy). Lewis et al. (2021) also found a strong association between point infiltration (measured with the double ring and the Cornell) and the hydraulic conductivity of saturated soil on the soil surface, but did not relate this to antecedent moisture.

The higher SIR measured with the Cornell than with the double ring is likely due to the greater lateral flow in the former compared to the latter method. For example, due to the absence of an outer ring in the Cornell, lateral infiltration may increase. However, if only the vertical component of infiltration of the Cornell tests were estimated with strategies proposed in the literature (e.g., Reynolds and Elrick, 1990; Stewart and Abou Najm, 2018), it would be similar to the SIR measured with the double ring, corroborating Lewis et al. (2021). Yet, Zwirtes et al. (2013) found the SIR measured with the double ring was greater than the SIR measured with the Cornell. That may have occurred because the hydraulic pressure head used in the double ring methodology by these authors (hydraulic pressure head = 0.04 to 0.05 m) was greater than the hydraulic pressure head used in the double ring methodology in this study (hydraulic pressure head = 0.03 m).

Regardless of the measurement method, the SIR obtained under antecedent moisture at or below field capacity was significantly higher than the Kef. At field capacity, for example, a condition in which recent studies measured infiltration with infiltrometers under tropical conditions (Boeno et al., 2021; Rauber et al., 2021), the relationship between the SIR and the Kef (SIR/Kef) in the areas with no-till and no-till with subsoiling was 3.1 and 8.2 in the double ring measurements and 5.7 and 15 in the Cornell measurements, respectively (Figure 2).

Our results suggest that under antecedent moisture at or below field capacity, the outer ring in the double concentric ring methodology does not completely eliminate the lateral flow from the inner ring (in which the infiltration readings are taken), which corroborates the assumptions of Bouwer (1986). However, the increase in antecedent soil moisture increased the efficiency of the outer ring in controlling the lateral flow from the inner ring (Figure 2). For example, for the subsoiled area and under nearly saturated soil (degree of saturation ~90 %), the SIR measured with the double ring drew near the Kef (Figure 2). In contrast, for the same structural condition and moisture level, but under measurement with Cornell (single ring), the SIR was ~ 8 times greater than the Kef (Figure 2).

The fact that extending the time of the test with the double ring (2 to 24 h and 48 h) does not generate a new lower level of the SIR (Figure 3) – especially at the points of high infiltration rate (such as the subsoiled area on April 19, 2022) – suggests that the main limiting factor for point infiltration measured with infiltrometers is the lateral flow component, especially if the antecedent moisture is sufficiently low (i.e., below field capacity) and/or the surface permeability to water is sufficiently high (e.g., in recently subsoiled areas) (Figures 2, 3, and 4). For example, in a soil profile with surface layers more permeable to water than the subsurface layers, when the vertical flow in infiltration measured with infiltrometers reaches the more restrictive layers (such as 0.20-0.40 m, Table 1), the lateral flow in the immediately higher layer (more permeable) is enhanced if the lateral hydraulic gradient – determined by antecedent moisture (matric potential) – is sufficiently high. For soil that is initially saturated or nearly saturated, in contrast, lateral infiltration is minimized, due to the low lateral hydraulic gradient.

In general, 2 h of the infiltration test with the double concentric ring was enough for the wetting front to reach the more restrictive layer of the water flow profile (0.20-0.40 m) (Figure 4). This measurement time was also enough for the wetting front to reach the Bt horizon at some points (Figure 4). Possibly some type of preferential flow through macropores (Nimmo, 2021) contributed to the relatively quick advance of the wetting front (Figure 4). Other authors (Boeno et al., 2021), for example, estimated that the time for the flow to reach the Bt horizon in soil with stratification and permeability to water similar to that of this study (and under antecedent moisture at field capacity), would be longer than 5 h. In any case, even increasing the testing time from 2 to 24 h and 48 h, there was not large enough dissipation of the lateral hydraulic gradient for the SIR to decrease in levels and tend towards the Kef (Figures 3 and 4). At a specific measuring point, the infiltration rate even increased after 15 h of testing (Figure 4c), perhaps through some type of disaggregation and increase in pore continuity during the test. However, that was an outlier in the database.

Another important observation from this study is that the saturation of the layers underlying the 0.20-0.40 m layer (except for the Bt horizon) during the infiltration process was incomplete (Figure 4). Furthermore, the changes in moisture at different depths during infiltration were more gradual than we expected (Figure 4). This may have resulted from the considerable hydraulic resistance of the 0.20-0.40 m layer (Table 1). For example, the flux density in this layer is not large enough to saturate the more permeable underlying layers (Figure 4). That also seems to occur in infiltration under natural rainfall. For example, the 0.30-m depth was frequently nearly saturated in natural rainfall events (Figure 1c). However, the 0.20-0.40 m layer limited the infiltration and saturation of the underlying layers (Figure 1c). Whereas at the depths of 0.15, 0.30, and 0.85 m (Bt) the degree of saturation frequently reached values around 90 to 100 % during infiltration, at the depths of 0.50 and 0.68 m (E), the degree of saturation reached values of at most 80 % (Figure 1c and Figure 4).

Several technical and practical implications can be obtained from this study. For example, measurement of infiltration with infiltrometers under antecedent moisture at or below field capacity (degree of saturation of ~63 %) leads to overestimation of vertical infiltration, especially if the permeability to water of the soil surface is high and the measurement method is single ring (e.g., Cornell infiltrometer). Consequently, this may lead to underestimation of the surface runoff depth and undersizing of surface runoff containment or channeling works. The maximum degree of saturation observed in the 0.00-0.40 m layer and under which the SIR potentially coincided with the Kef was ~90 %. Thus, the range of the degree of saturation of 90 and 100 % seems to be the most suitable for the SIR measured with infiltrometers to correspond to vertical infiltration. The SIR measured under antecedent moisture at or below field capacity better detects the effect of the soil structural condition on permeability to water of the soil surface. Disregarding the effect of antecedent moisture on the SIR, however, can confuse analysis

of the effect of the structural condition on permeability to water of the soil surface. That is because, in addition to affecting the soil pore system (Table 1), the structural condition also affects the antecedent soil moisture (Figure 1).

CONCLUSIONS

Steady infiltration rate (SIR) of water into the soil decreases with an increase in antecedent soil moisture, and this relationship depends on the permeability to water of the soil surface layers and on the measurement method. However, extending testing time with the double ring infiltrometer from 2 to 48 h did not lead to a new lower level of the SIR, regardless of the antecedent moisture.

In soil that is stratified regarding permeability to water, an initially saturated or nearly saturated (degree of saturation >90 %) soil profile is necessary for the SIR measured with infiltrometers to correspond to vertical infiltration. Without this condition, the water flow in saturated soil and in a single direction is best characterized by the effective vertical hydraulic conductivity for a saturated profile determined with Darcy's equation for N layers.

Subsoiling in no-till significantly increased the soil surface permeability to water and reduced water storage in the soil. These effects remained for at least 20 months. Nevertheless, subsoiling had little effect on the effective vertical hydraulic conductivity of the saturated profile.

The SIR measured with a double ring infiltrometer better corresponds to vertical infiltration than the SIR measured with a Cornell infiltrometer, especially if the permeability to water of the soil surface is high (e.g., no-till areas recently chiseled or subsoiled). However, despite their considerable capacity to detect soil surface permeability to water, measurement of point infiltration with infiltrometers has important limitations in adequately characterizing vertical infiltration of water into the soil.

DATA AVAILABILITY

The data will be provided upon request.

ACKNOWLEDGMENTS

SUPPLEMENTARY DATA

Supplementary data to this article can be found online at https://www.rbcsjournal.org/wp-content/uploads/articles_xml/1806-9657-rbcs-48-e0240007/1806-9657-rbcs-48-e0240007-suppl01.pdf.

AUTHOR CONTRIBUTIONS

Conceptualization: Dalvan José Reinert (equal), Lucas Raimundo Rauber (equal) and Paulo Ivonir Gubiani (equal).

Data curation: Lucas Raimundo Rauber (lead).

Formal analysis: Lucas Raimundo Rauber (lead).

Investigation: (iD) Dalvan José Reinert (equal), (iD) Lucas Raimundo Rauber (equal), (iD) Paulo Ivonir Gubiani (equal) and (iD) Suelen Matiasso Fachi((equal).

Methodology: (iD) Lucas Raimundo Rauber (lead).

Project administration: (iD) Lucas Raimundo Rauber (lead).

Supervision: (iD) Dalvan José Reinert (lead).

Validation: (iD) Lucas Raimundo Rauber (lead).

Visualization: (iD) Dalvan José Reinert (equal), (iD) Lucas Raimundo Rauber (equal), (iD) Paulo Ivonir Gubiani (equal) and (iD) Suelen Matiasso Fachi((equal).

Writing – original draft: (iD) Dalvan José Reinert (equal), (iD) Lucas Raimundo Rauber (equal), (iD) Paulo Ivonir Gubiani (equal) and (iD) Suelen Matiasso Fachi((equal).

REFERENCES

Assouline S. Infiltration into soils: Conceptual approaches and solutions. Water Resour Res. 2013;49:1755-72. https://doi.org/10.1002/wrcr.20155

Bertol I, Barbosa FT, Bertol C, Luciano RV. Water infiltration in two cultivated soils in southern Brazil. Rev Bras Cienc Solo. 2015;39:573-88. https://doi.org/10.1590/01000683rbcs20140304

Bodner G, Loiskandl W, Buchan G, Kaul HP. Natural and management-induced dynamics of hydraulic conductivity along a cover-cropped field slope. Geoderma. 2008;146:317-25. https://doi.org/10.1016/j.geoderma.2008.06.012

Bodner G, Scholl P, Loiskandl W, Kaul HP. Environmental and management influences on temporal variability of near saturated soil hydraulic properties. Geoderma. 2013;204-205:120-9. https://doi.org/10.1016/j.geoderma.2013.04.015

Boeno D, Gubiani PI, van Lier QJ, Mulazzani RP. Estimating lateral flow in double ring infiltrometer measurements. Rev Bras Cienc Solo. 2021;45:e0210027. https://doi.org/10.36783/18069657rbcs20210027

Bouwer H. Intake rate: Cylinder infiltrometer. In: Klute A, editor. Methods of soil analysis. Part 1. Physical and mineralogical methods. Madison: Soil Science Society of America; 1986. p. 825-44. https://doi.org/10.2136/sssabookser5.1.2ed.c32

Castiglioni MG, Sasal MC, Wilson M, Oszust JD. Seasonal variation of soil aggregate stability, porosity and infiltration during a crop sequence under no tillage. Terra Latinoam. 2018;36:199-206. https://doi.org/10.28940/terra.v36i3.333

Císlerová M, Šimůnek J, Vogel T. Changes of steady-state infiltration rates in recurrent ponding infiltration experiments. J Hydrol. 1988;104:1-16. https://doi.org/10.1016/0022-1694(88)90154-0

Cui Z, Wu GL, Huang Z, Liu Y. Fine roots determine soil infiltration potential than soil water content in semi-arid grassland soils. J Hydrol. 2019;578:124023. https://doi.org/10.1016/j.jhydrol.2019.124023

Drescher MS, Reinert DJ, Denardin JE, Gubiani PI, Faganello A, Drescher GL. Duração das alterações em propriedades físico-hídricas de Latossolo argiloso decorrentes da escarificação mecânica. Pesq Agropec Bras. 2016;51:159-68. https://doi.org/10.1590/S0100-204X2016000200008

Fundação Estadual de Proteção Ambiental - Fepam. Diretriz técnica referente ao descarte e ao reúso de efluentes líquidos no âmbito do estado do Rio Grande do Sul. Porto Alegre: Fepam; 2019.

Hillel D. Environmental soil physics. San Diego: Elsevier; 2003. https://doi.org/10.1016/B978-0-12-348655-4.X5000-X

Lewis JD, Amoozegar A, Mclauglin RA, Heitman JL. Comparison of cornell sprinkle infiltrometer and double-ring infiltrometer methods for measuring steady infiltration Rate. Soil Sci Soc Am J. 2021;85:1977-84. https://doi.org/10.1002/saj2.20322

Lili M, Bralts VF, Yinghua P, Han L, Tingwu L. Methods for measuring soil infiltration: State of the art. Int J Agric Biol Eng. 2008;1:22-30. https://doi.org/10.3965/j.issn.1934-6344.2008.01.022-030

Liu Y, Cui Z, Huang Z, López-Vicente M, Wu GL. Influence of soil moisture and plant roots on the soil infiltration capacity at different stages in arid grasslands of China. Catena. 2019;182:104147. https://doi.org/10.1016/j.catena.2019.104147

Nimmo JR. The processes of preferential flow in the unsaturated zone. Soil Sci Soc Am J. 2021;85:1-27. https://doi.org/10.1002/saj2.20143

Ogden CB, van Es HM, Shindelbeck R. Miniature rain simulator for field measurement of soil infiltration. Soil Sci Soc Am J. 1997;61:1041-3. https://doi.org/10.2136/sssaj1997.03615995006100040008x

Pedron FA, Lourenzi CR, Ceretta CA, Lorensi J, Cancian A. Clay mineralogy of subtropical soils under long-term organic fertilization in no-tillage systems. Rev Bras Cienc Solo. 2018;42:e0170092. https://doi.org/10.1590/18069657rbcs20170092

Philip JR. The theory of infiltration: 5- The influence of initial moisture content. Soil Sci. 1957;84:329-39.

Philip JR. Theory of infiltration. Adv Hydrosci. 1969;5:215-96. https://doi.org/10.1016/b978-1-4831-9936-8.50010-6

Pruski FF, Ferreira PA, Ramos MM, Cecon PR. Model to design level terraces. J Irrig Drain Eng. 1997;123:8-12. https://doi.org/10.1061/(asce)0733-9437(1997)123:1(8)

R Development Core Team. R: A language and environment for statistical computing. Vienna, Austria: R Foundation for Statistical Computing; 2022. Available from: http://www.R-project.org/.

Rahmati M, Weihermüller L, Vanderborght J, Pachepsky YA, Mao L, Sadeghi SH, Moosavi N, Kheirfam H, Montzka C, Van Looy K, Toth B, Hazbavi Z, Al Yamani W, Albalasmeh AA, Alghzawi MZ, Angulo-Jaramillo R, Antonino ACD, Arampatzis G, Armindo RA, Asadi H, Bamutaze Y, Batlle-Aguilar J, Béchet B, Becker F, Blöschl G, Bohne K, Braud I, Castellano C, Cerdà A, Chalhoub M, Cichota R, Císlerová M, Clothier B, Coquet Y, Cornelis W, Corradini C, Coutinho AP, Oliveira MB, Macedo JR, Durães MF, Emami H, Eskandari I, Farajnia A, Flammini A, Fodor N, Gharaibeh M, Ghavimipanah MH, Ghezzehei TA, Giertz S, Hatzigiannakis EG, Horn R, Jiménez JJ, Jacques D, Keesstra SD, Kelishadi H, Kiani-Harchegani M, Kouselou M, Kumar JM, Lassabatere L, Li X, Liebig MA, Lichner L, López MV, Machiwal D, Mallants D, Mallmann MS, Marques JDO, Marshall MR, Mertens J, Meunier F, Mohammadi MH, Mohanty BP, Pulido-Moncada M, Montenegro S, Morbidelli R, Moret-Fernández D, Moosavi AA, Mosaddeghi MR, Mousavi SB, Mozaffari H, Nabiollahi K, Neyshabouri MR, Ottoni MV, Ottoni Filho TB, Pahlavan-Rad MR, Panagopoulos A, Peth S, Peyneau P-E, Picciafuoco T, Poesen J, Pulido M, Reinert DJ, Reinsch S, Rezaei M, Roberts FP, Robinson D, Rodrigo-Comino J, Rotunno Filho OC, Saito T, Suganuma H, Saltalippi C, Sándor R, Schütt B, Seeger M, Sepehrnia N, Moghaddam ES, Shukla M, Shutaro S, Sorando R, Stanley AA, Strauss P, Su Z, Taghizadeh-Mehrjardi R, Taguas E, Teixeira WG, Vaezi AR, Vafakhah M, Vogel T, Vogeler I, Votrubova J, Werner S, Winarski T, Yilmaz D, Young MH, Zacharias S, Zeng Y, Zhao Y, Zhao H, Vereecken H. Development and analysis of the Soil Water Infiltration Global database. Earth Syst Sci Data. 2018;10:1237-63. https://doi.org/10.5194/essd-10-1237-2018

Rauber LR. Plantas de cobertura e umidade antecedente afetam a infiltração de água em um Argissolo [thesis]. Santa Maria:Universidade Federal de Santa Maria; 2023.

Rauber LR, Sequinatto L, Kaiser DR, Bertol I, Baldissera TC, Garagorry FC, Sbrissia AF, Pereira GE, Pinto CE. Soil physical properties in a natural highland grassland in southern Brazil subjected to a range of grazing heights. Agr Ecosyst Environ. 2021;319:107515. https://doi.org/10.1016/j.agee.2021.107515

Reinert DJ, Reichert JM. Coluna de areia para medir a retenção de água no solo – Protótipos e teste. Cienc Rural. 2006;36:1931-5. https://doi.org/10.1590/S0103-84782006000600044

Reynolds WD, Elrick DE. Ponded infiltration from a single Ring: I. Analysis of steady flow. Soil Sci Soc Am J. 1990;54:1233-41. https://doi.org/10.2136/sssaj1990.03615995005400050006x

Santos HG, Jacomine PKT, Anjos LHC, Oliveira VA, Lumbreras JF, Coelho MR, Almeida JA, Araújo Filho JC, Oliveira JB, Cunha TJF. Sistema brasileiro de classificação de solos. 5. ed. rev. ampl. Brasília, DF: Embrapa; 2018.

Sartori A, Genovez AM, Lombardi Neto F. Classificação hidrológica de solos brasileiros para a estimativa da chuva excedente com o método do Serviço de Conservação do Solo dos Estados Unidos Parte 2: Aplicação. Rev Bras Recur Hídricos. 2005b;10:19-29. https://doi.org/10.21168/rbrh.v10n4.p19-29

Sartori A, Lombardi Neto F, Genovez AM. Classificação hidrológica de solos brasileiros para a estimativa da chuva excedente com o método do Serviço de Conservação do Solo dos Estados Unidos Parte 1: Classificação. Rev Bras Recur Hídricos. 2005a;10:5-18. https://doi.org/10.21168/rbrh.v10n4.p5-18

Seratto CD, Franchini JC, Seratto FR, Debiasi H, Santos EL, Conte O, Neto SM, Brischiliari V. Infiltrômetro de aspersão de Cornell aperfeiçoado: aspectos construtivos, operacionais e de manutenção. Londrina: Empresa Brasileira de Pesquisa Agropecuária; 2019.

Soil Survey Staff. Keys to soil taxonomy. 13th ed. Washington, DC: United States Department of Agriculture, Natural Resources Conservation Service; 2022.

Stewart RD, Najm MRA. A comprehensive model for single ring infiltration II: Estimating field-saturated hydraulic conductivity. Soil Sci Soc Am J. 2018;82:558-67. https://doi.org/10.2136/sssaj2017.09.0314

Teixeira PC, Donagemma GK, Fontana A, Teixeira WG. Manual de métodos de análise de solo. 3. ed. rev e ampl. Brasília, DF: Embrapa; 2017.

van Es H, Schindelbeck R. Field procedures and data analysis for the cornell sprinkle infiltrometer. Ithaca, NY: Cornell University. College of Agriculture and Life Scinces. Department of Crop and Soil Sciences; 2003.

Wei L, Yang M, Li Z, Shao J, Li L, Chen P, Li S, Zhao R. Experimental investigation of relationship between infiltration rate and soil moisture under rainfall conditions. Water. 2022;14:1347. https://doi.org/10.3390/w14091347

Yang M, Zhang Y, Pan X. Improving the Horton infiltration equation by considering soil moisture variation. J Hydrol. 2020;586:124864. https://doi.org/10.1016/j.jhydrol.2020.124864

Zwirtes AL, Spohr RB, Baronio CA, Menegol DR, da Rosa GM, de Moraes MT. Utilização do infiltrômetro de Cornell e dos anéis concêntricos para determinação da infiltração de água em um Latossolo Vermelho. Semin-Cienc Agrar. 2013;34:3489-500. https://doi.org/10.5433/1679-0359.2013v34n6Supl1p3489